Neurobiology of Disease 151 (2021) 105271

Contents lists available at ScienceDirect

Neurobiology of Disease

journal homepage: www.elsevier.com/locate/ynbdi

T_1AM-TAAR1 signalling protects against OGD-induced synaptic dysfunction in the entorhinal cortex

Francesca Tozzi [a], Grazia Rutigliano [b], Marco Borsò [b], Chiara Falcicchia [c], Riccardo Zucchi [b], Nicola Origlia [c,*]

[a] Bio@SNS laboratory, Scuola Normale Superiore, 56124 Pisa, Italy
[b] Department of Pathology, University of Pisa, 56100 Pisa, Italy
[c] Institute of Neuroscience of the Italian National Research Council (CNR), Pisa, Italy

ARTICLE INFO

Keywords:
3-iodothyronamine
Trace amine-associated receptor 1
Synaptic depression
Ischemia
Entorhinal cortex
Brain derived neurotrophic factor
Alzheimer's disease

ABSTRACT

Abnormalities in thyroid hormones (TH) availability and/or metabolism have been hypothesized to contribute to Alzheimer's disease (AD) and to be a risk factor for stroke. Recently, 3-iodothyronamine (T_1AM), an endogenous amine putatively derived from TH metabolism, gained interest for its ability to promote learning and memory in the mouse. Moreover, T_1AM has been demonstrated to rescue the β-Amyloid dependent LTP impairment in the entorhinal cortex (EC), a brain area crucially involved in learning and memory and early affected during AD. In the present work, we have investigated the effect of T_1AM on ischemia-induced EC synaptic dysfunction. In EC brain slices exposed to oxygen-glucose deprivation (OGD), we demonstrated that the acute perfusion of T_1AM (5 μM) was capable of preventing ischemia-induced synaptic depression and that this protective effect was mediated by the trace amine-associated receptor 1 (TAAR1). Moreover, we demonstrated that activation of the BDNF-TrkB signalling is required for T_1AM action during ischemia. The protective effect of T_1AM was more evident when using EC slices from transgenic mutant human APP (mhAPP mice) that are more vulnerable to the effect of OGD. Our results confirm that the TH derivative T_1AM can rescue synaptic function after transient ischemia, an effect that was also observed in a Aβ-enriched environment.

1. Introduction

Stroke is one of the leading causes of death, and in most cases it is caused by brain ischemia. In addition, cerebral ischemia has been suggested to contribute to other neurological diseases, including Alzheimer's Disease (AD). Although a causal relationship between AD and brain ischemia remains to be established, common pathogenic mechanisms between ischemia and neurodegeneration have been suggested (Girouard and Iadecola, 2006). In particular, hypoxia has been shown to increase the expression of the amyloid-beta (Aβ) precursor protein (APP), enhance Aβ cleavage and slow down Aβ clearance (Abe et al., 1991; Uryu et al., 2002; Yokota et al., 1996), leading to an early impairment of cognitive functions during AD (Zhang et al., 1997). Furthermore, enhanced vulnerability to ischemia has been observed in the brains of APP-overexpressing mice (Origlia et al., 2014).

Among the neuromodulatory and neuroendocrine systems able to regulate neuronal and vascular function, thyroid hormones (TH) gained interest as they appear to play a pathophysiological role in both degenerative and ischemic disease. In fact, abnormalities in TH availability and/or metabolism have been hypothesized to contribute to AD and to be a risk factor for stroke (Bai et al., 2014; Cummings et al., 1980; Gao et al., 2013; Iwen et al., 2013; O'Barr et al., 2006; Smith and Kiloh, 1981). In preclinical studies, TH administration was found to protect hippocampal neurons from ischemia-induced damage and glutamate-

Abbreviations: aCSF, artificial cerebrospinal fluid; AD, Alzheimer's disease; APP, amyloid precursor protein; Aβ, amyloid beta peptide; BDNF, brain-derived neurotrophic factor; EC, entorhinal cortex; EPPTB, N-(3-ethoxyphenyl)-4-(pyrrolidin-1-yl)-3 trifluoromethylbenzamide; fEPSP, field excitatory post-synaptic potential; HPLC, high performance liquid chromatography; IgG, immunoglobulin G; LC, liquid chromatography; LTP, long-term potentiation; mhAPP, mutant human amyloid precursor protein; MS, mass spectrometry; OGD, oxygen-glucose deprivation; PI3K, phosphoinositide-3-kinase; T_1AM, 3-iodothyronamine; T_3, triiodothyronine; TA_1, 3-iodothyroacetic acid; TAAR1, trace amine-associated receptor 1; TH, thyroid hormone; TR, thyroid hormone receptor; TrkB, tropomyosin receptor kinase B.

* Corresponding author at: Institute of Neuroscience of the Italian National Research Council (CNR), Via Moruzzi 1, Pisa 56124, Italy
E-mail address: origlia@in.cnr.it (N. Origlia).

https://doi.org/10.1016/j.nbd.2021.105271
Received 11 August 2020; Received in revised form 4 December 2020; Accepted 15 January 2021
Available online 19 January 2021

induced death through a non-genomic mechanism involving *N*-methyl-D-aspartate (NMDA) receptors (Losi et al., 2008). Moreover, TH are reported to modulate APP transcription and processing (Belakavadi et al., 2011) and to rescue memory deficits and related morphological and electrophysiological alterations in rodent models of AD (Farbood et al., 2017).

The relationship between hypothyroidism and AD in humans remains elusive, although several investigations described altered hormonal levels of TH and/or thyroid stimulating hormone (TSH) – in the serum, cerebrospinal fluid or post-mortem brains of patients suffering from dementia (Accorroni et al., 2017; Ganguli et al., 1996; Johansson et al., 2013; Sampaolo et al., 2005; Volpato et al., 2002). It is becoming increasingly clear that TH have a complex metabolism and their central effect can be mediated by a composite network of metabolites. In particular, 3-iodothyronamine (T_1AM), a novel endogenous TH derivative discovered by Scanlan et al. (Scanlan et al., 2004), gained interest for its ability to modulate both the nervous and the vascular system. T_1AM was initially described to have a negative ionotropic and chronotropic effect (Chiellini et al., 2007). While these actions occurred at pharmacological dosages, much lower concentrations exerted a protective effect against the ischemia-reperfusion injury (Frascarelli et al., 2011). Concerning the nervous system, T_1AM i.c.v. injection has been shown to modulate sleep and feeding behaviour and to promote learning and memory in mice (Hoefig et al., 2016; Köhrle and Biebermann, 2019; Manni et al., 2013; Zucchi et al., 2014). In addition, T_1AM demonstrated neuroprotective activity in several models, including seizure-related excitotoxic damage, altered autophagy, and amyloidosis (Bellusci et al., 2017; Landucci et al., 2019). In particular, we have previously shown that T_1AM and other agonists of TAAR1, its putative receptor, rescue Aβ-induced synaptic and behavioural dysfunctions in a mouse model of AD. T_1AM administration *in vitro* and *in vivo* led to a complete rescue of the electrophysiological and behavioural abnormalities in transgenic APP swe/Ind J20 mice (mhAPP), at an early stage of neurodegeneration (Accorroni et al., 2019).

Based on this evidence and on the possibility that AD and ischemia could share at least some pathological mechanisms, in the present work we investigated whether T_1AM could have a protective role against the ischemia-induced synaptic failure both in WT brain slices and in an amyloid-enriched environment, namely brain slices obtained from mhAPP mice. We focused on the EC, a brain region early affected during AD (Braak and Braak, 1995) and particularly vulnerable to ischemia in the presence of Aβ (Criscuolo et al., 2017).

2. Materials and methods

2.1. Animals

Transgenic mhAPP mice (APPsweInd, line J20) overexpressing an alternatively spliced human APP minigene that encodes hAPP695, hAPP751, and hAPP770 bearing mutations linked to familial AD (V717F, K670N/M671L) (Mucke et al., 2000) were used together with their littermates. Transgenic mhAPP mice were obtained from Jackson Laboratories (Maine, USA) and mice were bred and mated with wild-type mice (C57BL/6 J). Experiments were performed in animals of 4–5 months of age, in accordance with the Italian Ministry of Health and the European Community guidelines (Legislative Decree n. 116/92 and European directive 86/609/EEC). The experimental protocol (IACUC document) was approved by the Ministry of Health (protocol n. 192/2000-A and n.74/2017).

2.2. Drugs

T_1AM and the TAAR1 antagonist N-(3-ethoxyphenyl)-4-(pyrrolidin-1-yl)-3 trifluoromethylbenzamide (EPPTB) were purchased from Sigma-Aldrich (St.Louis, MO); the TAAR1 agonist (*S*)-4-[(ethylphenylamino) methyl]-4,5-dihydrooxazol-2-ylamine (RO5166017) was kindly provided by Dr. Gainetdinov. Aliquots were stored at −20 °C in DMSO as a 200 mM stock solution and diluted to the desired final concentration in artificial CSF (aCSF). The aCSF was prepared as follows (in mM): 119 NaCl, 2.5 KCl, 2 $CaCl_2$, 1.2 $MgSO_4$, 1 NaH_2PO_4, 6.2 $NaHCO_3$, 10 HEPES and 11 glucose. T_1AM (5 μM), RO5166017 (250 nM), EPPTB (5 nM), recombinant human BDNF (1 ng/ml, recombinant human BDNF, QED, USA) and LY294002 (PI3K specific inhibitor, 10 nM, Cell Signalling, Leiden, NL) were applied during OGD, while anti-TrkB antibodies (1 μg/ml, Santa Cruz Biotechnology, TX, USA) and TrkB-IgGs (1 μg/ml; rhTrkB/Fc Chimera, R&D Systems, USA) were administered to slices before the electrophysiological recording, allowing them to incubate for 2 h. All drugs were administered at concentrations previously demonstrated not to alter basic synaptic transmission in the EC (Accorroni et al., 2019).

In vitro electrophysiology. Electrophysiology was performed as in (Origlia et al., 2010; Origlia et al., 2009; Origlia et al., 2008). Mice were deeply anesthetized with urethane i.p. (20% solution, 0.1 ml/100 g of body weight) and then decapitated after disappearance of the tail pinch reflex. The brain was rapidly removed and thick horizontal sections (400 μm) containing the entorhinal area were obtained using a vibratome (Leica VT1200S). All steps were performed in ice-cold oxygenated aCSF. Slices were stored for at least 1 h in a recovery chamber containing oxygenated aCSF solution at room temperature. Then, slices were transferred to a chamber and perfused at 2–3 ml/min rate with oxygenated aCSF at 33 ± 1 °C. Field excitatory postsynaptic potentials (fEPSPs) were evoked by a concentric bipolar stimulating electrode in the layer II of the EC. The amplitude of the fEPSPs was used as a measure of the evoked population excitatory current. All fEPSPs had a peak latency between 4.5 and 6.5 ms. Baseline responses were obtained with a stimulation intensity that yielded 50–60% of maximal amplitude. After 10 min of stable baseline recordings, slices were perfused for 10 min with deoxygenated glucose-free aCSF (glucose was substituted with D-mannitol at equimolar concentration) to obtain a transient OGD. The amplitude of fEPSP was monitored every 20 s and averaged every three responses by online data acquisition software. Effects on synaptic function were evaluated both during ischemia (as the average of fEPSP amplitude during the last 3 min of 10 min OGD application) and as the recovery of fEPSPs amplitude (averaged fEPSPs amplitude from minutes 41–50 after the end of OGD and reintroduction of regular aCSF).

2.3. ELISA

After the electrophysiological recordings, slices were collected to measure BDNF protein levels. BDNF was detected using an ELISA kit (Promega, USA). In brief, 96-well plates were coated with an anti-BDNF monoclonal antibody and incubated at 4 °C for 18 h. The plates were incubated in a blocking buffer for 1 h at room temperature and then the samples were added. Tissue extracts were prepared using the lysis buffer described in the Promega protocol. Samples were then diluted with the Block and Sample solution. The samples and BDNF standards were incubated for 2 h, followed by washing with the appropriate buffer. Plates were incubated with anti-human BDNF polyclonal antibody at room temperature for 2 h, then washed and incubated with anti-IgG antibody conjugated to horseradish peroxidase for 1 h at room temperature. Finally, the plates were incubated in peroxidase substrate and tetramethylbenzidine solution to produce colour reaction. The reaction was stopped with 1 M HCl. The absorbance was measured at 450 nm using a microplate reader (Model 550, Bio Rad Laboratories). Total protein levels were assessed by Bradford protein assay and BDNF levels were expressed as pg/mg of protein.

2.4. Analysis of T_1AM and TA_1

T_1AM and its metabolite 3-iodothyroacetic acid (TA_1) were assayed in aCSF samples by tandem mass spectrometry coupled to liquid chromatography (LC-MS-MS) as described by (Accorroni et al., 2019).

Effluent aCSF was collected over different time intervals during the whole duration of experiments. Aliquots (0.1 ml) from each collection were then spiked with 10 μl of a suitable mixture of internal standards (deuterated T_1AM and TA_1). After adding methanol (0.4 ml) the samples were shaken for 10 min and centrifuged at 22780 xg for 10 min. The supernatant was dried under a gentle stream of nitrogen, reconstituted with water/methanol mixture (70/30 by volume) and injected into the LC-MS-MS system. The latter included an Agilent 1290 UHPLC system (Santa Clara, CA, USA) coupled to an AB-Sciex API 4000 triple quadrupole mass spectrometer (Concord, Ontario, Canada). HPLC conditions and mass spectrometry settings were the same as in (Accorroni et al., 2019). Before each experiment, blank samples were collected by washing the perfusion system with standard aCSF (without any addition) and used to correct the results of the assay.

2.5. Statistical analysis

All data are reported as mean ± SEM. Statistical comparisons between experimental groups or between fEPSP amplitudes measured during baseline and after OGD protocol were performed by applying two-way repeated-measures ANOVA. A one-way repeated-measures ANOVA was used to analyse differences in the release of metabolites and T_1AM. For the analysis of the BDNF levels measured by ELISA we applied one-way ANOVA. Holm–Sidak method was used for multiple comparisons. Differences were considered significant when $p < 0.05$.

3. Results

3.1. T_1AM protects against OGD-induced synaptic dysfunction in the mouse EC

In order to investigate the effect of T_1AM on ischemia-induced synaptic dysfunction, we performed extracellular electrophysiological recordings in horizontal EC slices exposed to OGD (Fig. 1a). Recordings of fEPSPs in EC slices showed a significant effect of transient ischemia on synaptic function in the intrinsic circuitry of the EC. Indeed, a rapid fall of fEPSPs amplitude was observed in EC slices immediately after the application of OGD (mean relative fEPSP amplitude during OGD was 56 ± 9% of baseline, $n = 12$, 9 mice $p < 0.001$ *vs* baseline; Fig. 1b) and the fEPSPs amplitude only partially recovered at the end of the reperfusion, reaching a stable level of depression after 50 min (mean relative fEPSP amplitude 78 ± 4% of baseline, n = 12, 9 mice p < 0.001 *vs* baseline; Fig. 1b). The exogenous application of T_1AM (5 μM) during 10 min OGD did not affect the rapid fall in fEPSP amplitude induced by ischemia,

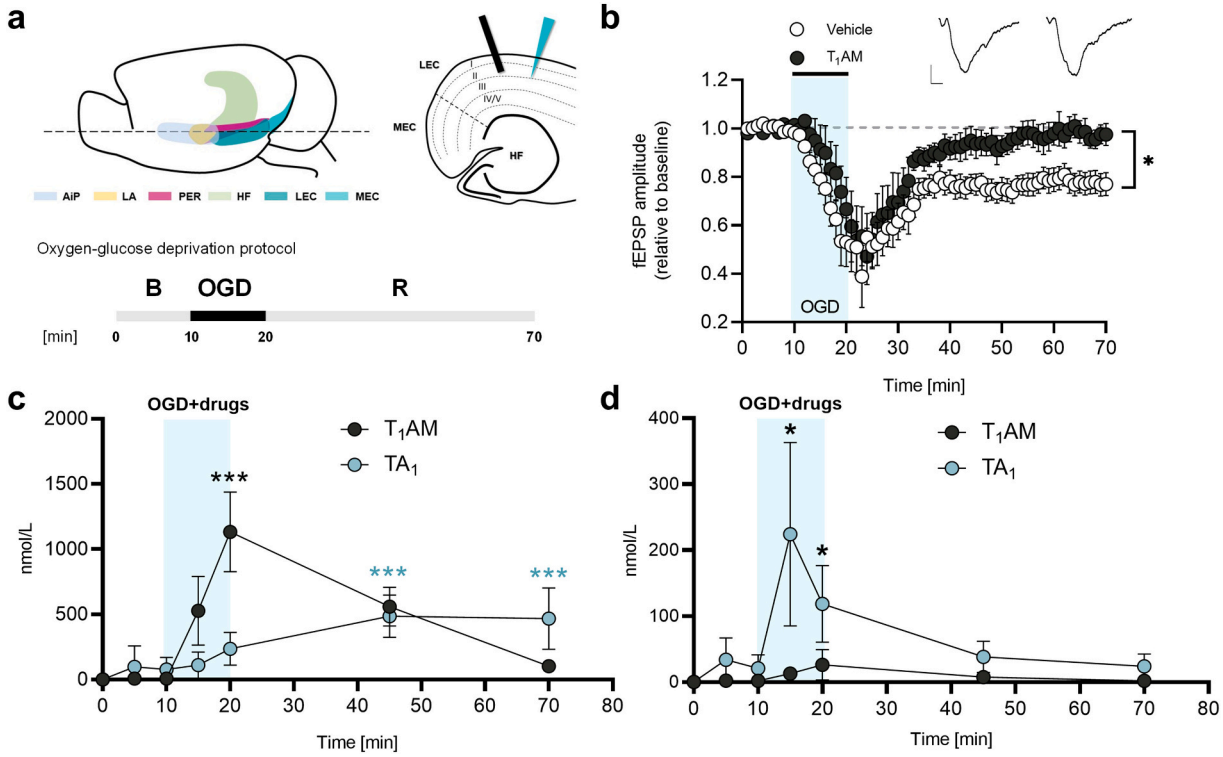

Fig. 1. Exogenous T_1AM administration protects against OGD-induced synaptic dysfunction in the mouse EC (a) Schematic representation of the lateral view of the mouse brain showing: the agranular insular cortex (AiP), the lateral amygdala (LA), the perirhinal cortex (PER), the hippocampal formation (HF), the lateral entorhinal (LEC) and the medial entorhinal cortex (MEC). The dotted line indicates the cut performed to obtain horizontal EC slices used for electrophysiology. Slices were recorded from the superficial layers of the EC while exposed to an oxygen-glucose deprivation (OGD) protocol composed by 10 min of baseline (B) in which slices were perfused with oxygenated aCSF, 10 min of ischemia (OGD) in which slices were perfused with glucose-free deoxygenated aCSF, 50 min of reperfusion (R) with the reintroduction of oxygenated aCSF. (b) The application of 10 min OGD induced a decrease in fEPSP amplitude in vehicle-treated slices and a significant long-term synaptic depression at the end of the reperfusion (white circles), while 5 μM T_1AM-treated slices showed a rapid fall in fEPSP amplitude following OGD and a complete recovery of fEPSP amplitude at the end of the reperfusion (black circles). The post-hoc comparison of vehicle and T_1AM mean fEPSP amplitude reached at the end of the reperfusion showed a significant difference between vehicle- and T_1AM-treated slices. The shaded area on the plot indicates the application time of OGD and the dark bar indicates the timeline of drug application. Inserts show typical traces of fEPSP recordings during the baseline and at the end of the reperfusion in T_1AM-treated slices (scale bar vert. = 0.2 mV, hor. = 2 ms). Error bars indicate SEM. Two-way ANOVA repeated measures and Holm-Sidak method for post-hoc multiple comparisons, ns = not significant, $*p < 0.05$. (c-d) Eluate T_1AM and TA_1 concentration (mean ± SEM of 5 different experiments). The eluate was divided into fractions collected over 5–25 min intervals, which were sampled for T_1AM and TA_1 by LC-MS-MS, as detailed in the text. Data are plotted at time points corresponding to the end of each interval. (c) Results of experiments with administration of exogenous T_1AM (5 μM) during OGD. $***p < 0.001$ *vs* time 0, dark asterisks refer to T_1AM, light asterisks to TA_1. (d) Results of control experiments, in which slices were perfused with standard aCSF (no T_1AM addition); $*p < 0.05$ *vs* time 0, asterisks refer to TA_1. Please note the different scale *vs* the (c) panel.

however it was able to completely recover fEPSPs amplitude at the end of the OGD protocol, preventing the long-lasting synaptic depression observed in vehicle treated slices (mean relative fEPSP amplitude in T_1AM-treated slices was 98 ± 5%, $n = 8$, 5 mice $p > 0.05$ *vs* baseline; $p = 0.024$ *vs* 78 ± 4%, $n = 12$, 9 mice in vehicle-treated slices; Fig. 1b). Therefore, we demonstrated that the pharmacological administration of T_1AM is capable of acting as a protective mechanism against the synaptic failure observed after a period of transient ischemia and reperfusion.

3.2. T_1AM distribution and metabolism

In our experimental setting, the nominal concentration of T_1AM in the perfusion medium does not correspond to the effective concentration reaching the cellular receptors, because of the combined effects of protein binding, cellular uptake and tissue metabolism (Hoefig et al., 2016). Since the perfusion buffer eluted from brain slices is assumed to be in equilibrium with the extracellular fluid (Accorroni et al., 2019), we collected it over 5 min periods up to the end of OGD, and over 25 min periods at reoxygenation, to assay the actual concentrations of T_1AM and its metabolite TA_1. During T_1AM perfusion (Fig. 1c), T_1AM concentration in the effluent increased up to 527 ± 118 and 1133 ± 137 nmol/l in the 10–15 and 15–20 min interval, respectively. In the same interval samples, TA_1 was detected at concentration averaging 110 ± 20 and 235 ± 25 nmol/l, respectively. In the washout phase, both T_1AM and TA_1 were detected in the effluent. In the 20–45 and 45–70 min samples, T_1AM concentration decreased from 559 ± 67 to 103 ± 11 nmol/l, while TA_1 concentration averaged 485 ± 32 and 468 ± 47 nmol/l, respectively. No other known T_1AM metabolite (namely the deiodinated derivatives thyronamine and thyroacetic acid) was observed. Thus, brain slices apparently take up exogenous T_1AM, which is progressively released either unchanged or after oxidation to TA_1. Local T_1AM concentration undergoes phasic changes, and it is 5-fold to 50-fold lower than the administered concentration, whereas TA_1 is on the same order as T_1AM concentration.

Notably, minimum but significant TA_1 release was observed also in control experiments during OGD. As shown in Fig. 1d, at the baseline a very low release of T_1AM or TA_1 was detected, which did not reach the threshold of statistical significance, and might be due to minimal contamination of the perfusion system with exogenous T_1AM. During OGD, T_1AM and TA_1 concentrations reached 26 ± 10 and 224 ± 62 nmol/l, respectively ($P < 0.05$ *vs.* time zero for TA_1), with progressive decrease after reoxygenation ($P < 0.05$ *vs.* time zero for TA_1 in the first reoxygenation period).

3.3. Specificity of T_1AM protection

Since TA_1 has been reported to be responsible for some effects elicited after the administration of exogenous T_1AM (Laurino et al., 2018; Laurino et al., 2015; Musilli et al., 2014), we checked whether in our experimental model TA_1 administration could also protect against OGD-induced synaptic dysfunction. We observed that the acute administration of TA_1 (5 μM) was not sufficient to protect against OGD-induced synaptic dysfunction. In fact, TA_1-treated slices showed a decrease in synaptic amplitude following ischemia (mean relative fEPSP amplitude 46 ± 11% of baseline, $n = 7$, 5 mice $p < 0.001$ *vs* baseline; Fig. 2a) and a long-term depression of synaptic transmission that was similar to what observed in vehicle-treated slices (mean relative fEPSP amplitude 61 ± 8% of baseline, n = 7, 5 mice $p > 0.05$ *vs* 78 ± 4%, $n = 12$, 9 mice, in vehicle-treated slices; Fig. 2a-c) suggesting that the neuroprotective action is mediated by T_1AM itself.

T_1AM has been hypothesized to derive from T_3 (Hoefig et al., 2016; Köhrle and Biebermann, 2019) and TH have been demonstrated to exert a protective role in ischemic injury. Therefore, we also investigated whether the administration of T_3 (5 μM) could have a similar protective effect against OGD. EC slices treated with T_3 showed a significant fall in

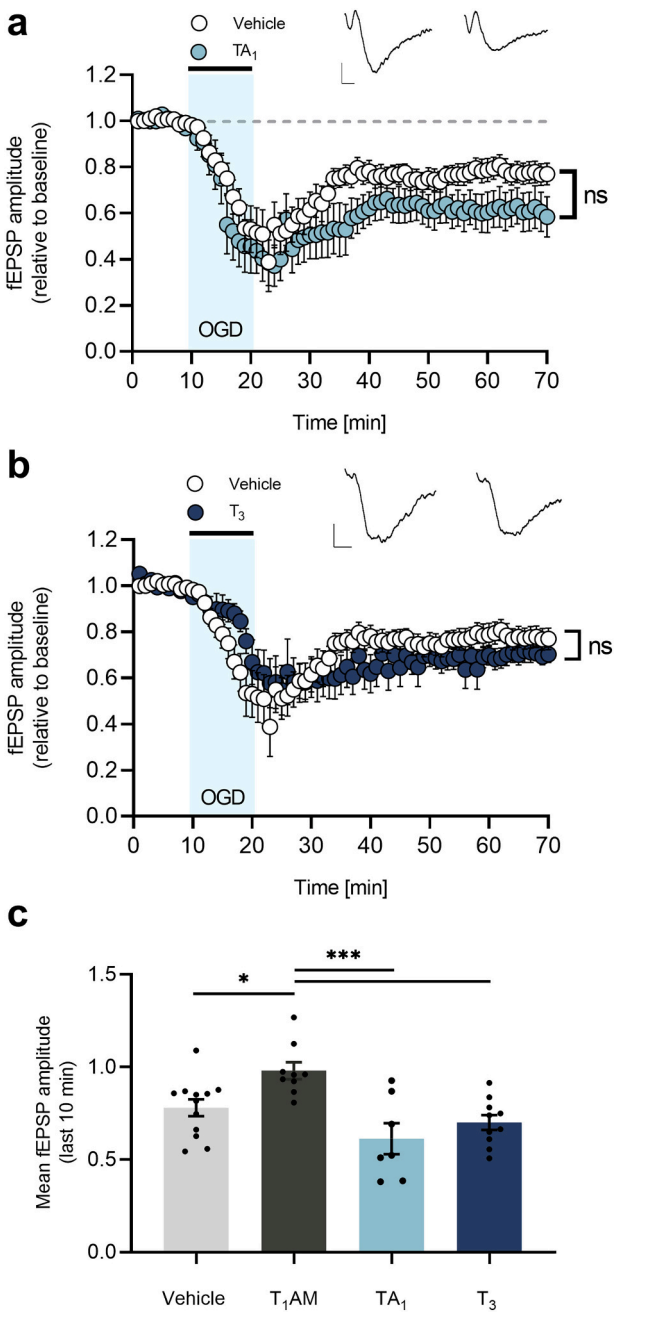

Fig. 2. T_1AM main metabolite (TA_1) and putative precursor (T_3) do not protect against OGD. (a) Ten min OGD induced a rapid fall in fEPSP amplitude in TA_1 (5 μM)-treated slices and a significant synaptic depression at the end of the reperfusion (dark circles). The post-hoc comparison of vehicle (white circles) and TA_1-treated slices mean fEPSP amplitudes at the end of the reperfusion showed no significant difference. (b) Ten min OGD induced a rapid fall in fEPSP amplitude in T_3 (5 μM)-treated slices and a significant synaptic depression at the end of the reperfusion (dark circles). The post-hoc comparison of vehicle (white circles) and T_3-treated slices mean fEPSP amplitudes at the end of the reperfusion showed no significant difference. The shaded areas on (a,b) plots indicate the application time of OGD and the dark bars indicate the timeline of drugs application. Inserts in (a,b) show typical traces of fEPSP recordings during the baseline and at the end of the reperfusion (scale bar vert. = 0.2 mV, hor. = 2 ms). Error bars indicate SEM. Two-way ANOVA repeated measures and Holm-Sidak method for post-hoc multiple comparisons, ns = not significant, *$p < 0.05$. (c) Summary histogram showing all significant pairwise multiple comparisons between groups (two-way ANOVA repeated measures, *post hoc* Holm-Sidak method. ns = not significant, *p < 0.05, ***$p < 0.001$). Error bars indicate SEM.

synaptic transmission following ischemia and an OGD-induced synaptic depression (mean fEPSP amplitude 70 ± 4% of baseline, $n = 10$, 5 mice, $p < 0.001$ *vs* baseline; Fig. 2b) comparable to that observed in vehicle-treated ones (mean relative fEPSP amplitude 70 ± 4% of baseline, n = 10, 5 mice, $p > 0.05$ *vs* 78 ± 4%, n = 12, 9 mice, in vehicle treated slices; Fig. 2b-c), suggesting that T_3 is not able protect against ischemia-induced synaptic function in our *in vitro* model. Notably, in pilot experiments, no release of T_1AM or TA_1 was observed when EC slices were perfused with 5 μM T_3.

3.4. TAAR1 is involved in T_1AM-mediated synaptic protection

The evidence that T_1AM has a protective effect against the ischemia-induced synaptic dysfunction prompted us to extend our investigation to its mechanism of action. It is known from the literature that T_1AM doesn't bind the nuclear TH receptors (TR) but it is a high-affinity ligand for the trace amine-associated receptors (TAARs), in particular for TAAR1 (Scanlan et al., 2004). However, T_1AM may interact with additional molecular targets, including other aminergic receptors, transient receptor potential channels, and membrane transporters (Hoefig et al., 2015; Köhrle et al., 2019). In our previous work, TAAR1 was found to be expressed at comparable levels in the EC of both WT and mhAPP mice and to co-localize with the neuronal marker NeuN (Accorroni et al., 2019). Moreover, TAAR1 was demonstrated to mediate T_1AM protective effect against synaptic plasticity abnormalities and to be a chief target of T_1AM in the mouse EC. Therefore, we investigated whether TAAR1 could play a role in our model of transient ischemia by using a TAAR1 selective antagonist (EPPTB) and a selective agonist (RO5166017). Interestingly, we observed that T_1AM protective effect was abolished by the co-perfusion of EPPTB (5 nM) to EC slices. In fact, slices treated with T_1AM and EPPTB showed a rapid fall in fEPSP amplitude following OGD (mean relative fEPSP amplitude 57 ± 12% of baseline, $n = 9$, 6 mice $p < 0.001$ *vs* baseline; Fig. 3a) and a long-term synaptic depression significantly different from that recorded in T_1AM-treated slices (mean relative fEPSP amplitude in EPPTB+T_1AM-treated slices was 77 ± 6% of baseline, n = 9, 6 mice $p < 0.001$ *vs* baseline and $p = 0.025$ *vs* 98 ± 5%, $n = 8$, 5 mice, in T_1AM treated slices; Fig. 3a-d). Moreover, the administration of EPPTB (5 nM) alone did not affect the ischemia-induced synaptic dysfunction and EPPTB-treated slices showed a long-term depression similar to vehicle-treated slices (mean relative fEPSP amplitude in

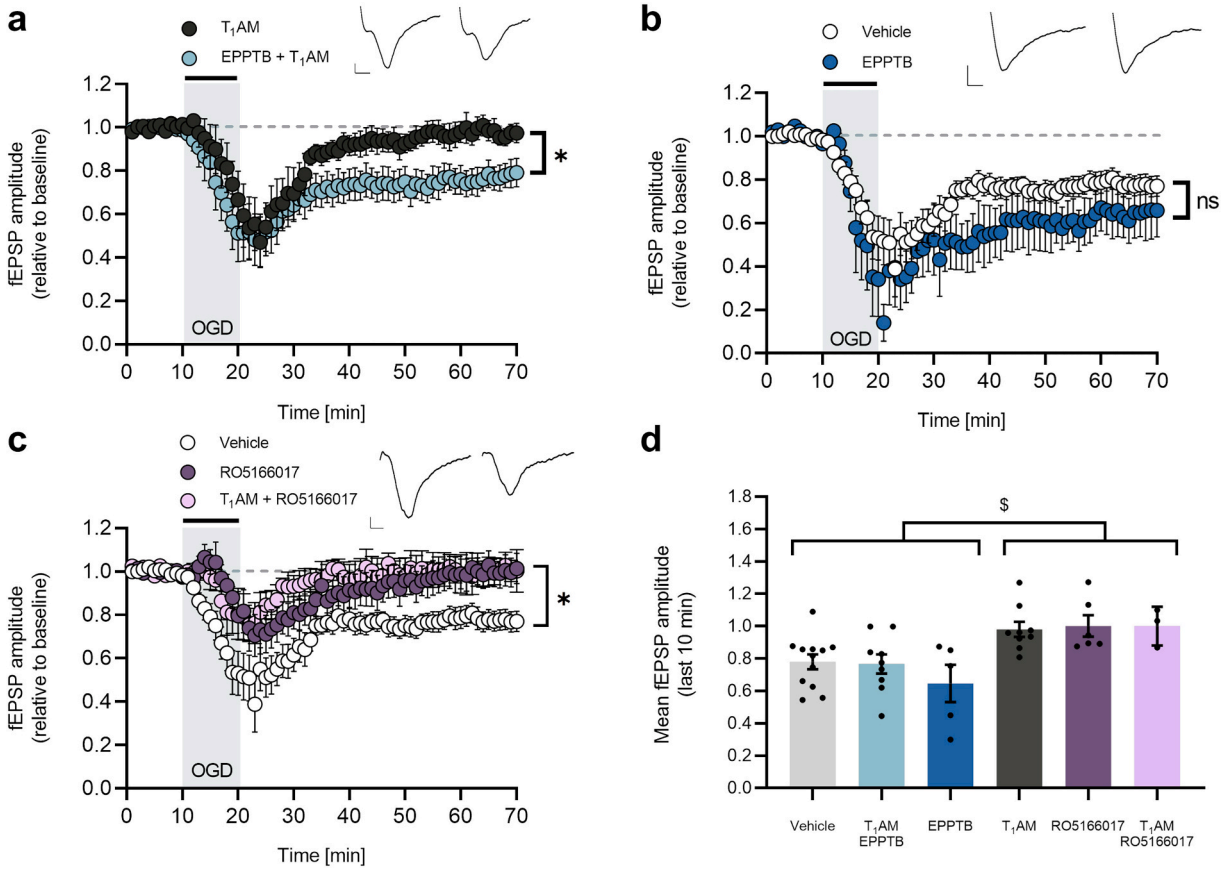

Fig. 3. TAAR1 involvement in T1AM-mediated synaptic protection against OGD. (a) EC slices co-perfused with T_1AM (5 μM) and the TAAR1 antagonist EPPTB (5 nM) showed a rapid fall in synaptic amplitude following OGD and a long-term depression at the end of the reperfusion significantly different from T_1AM-treated slices (black circles). (b) EC slices perfused with EPPTB (5 nM, dark circles) showed a rapid fall in synaptic amplitude following OGD and a long-term depression at the end of the reperfusion, similar to vehicle-treated slices (white circles). (c) EC slices treated with the TAAR1 agonist RO5166017 (250 nM, dark circles) showed a significant decrease in synaptic amplitude induced by OGD but they completely recover at the end of the reperfusion, showing a mean relative fEPSP amplitude significantly different from vehicle-treated slices (white circles). The same effect was observed following concomitant application of T_1AM (5 μM) and RO5166017 (250 nM; light circles). The shaded areas on (a,b,c) plots indicate the application time of OGD and the dark bars indicate the timeline of drugs application. Inserts in (a,b,c) show typical traces of fEPSP recordings during the baseline and at the end of the reperfusion (scale bar vert. = 0.2 mV, hor. = 2 ms). Error bars indicate SEM. Two-way ANOVA repeated measures and Holm-Sidak method for post-hoc multiple comparisons, ns = not significant, $^*p < 0.05$. (d) Summary histogram showing all significant pairwise multiple comparisons between groups (two-way ANOVA repeated measures, *post hoc* Holm-Sidak method, $ = statistically significant differences); Mean fEPSP 78 ± 4% of baseline in vehicle-treated slices $p < 0.05$ *vs* 98 ± 5% in T_1AM-treated slices, $p < 0.05$ *vs* 100 ± 7% of baseline in RO5166017-treated slices, $p < 0.05$ *vs* 100 ± 7% of baseline in T_1AM + RO5166017-treated slices; mean fEPSP 77 ± 6% of baseline in T_1AM + EPPTB-treated slices $p < 0.05$ *vs* T_1AM-treated slices, RO5166017-treated slices and T_1AM + RO5166017-treated slices; mean fEPSP 71 ± 11% of baseline in EPPTB-treated slices $p < 0.01$ *vs* T_1AM-treated slices,RO5166017-treated slices and T_1AM + RO5166017-treated slices. Error bars indicate SEM.

EPPTB-treated slices was 65 ± 10% of baseline, $n = 5$, 3 mice $p < 0.001$ *vs* baseline and $p > 0.05$ *vs* 78 ± 4%, $n = 12$, 9 mice, in vehicle-treated slices; Fig. 3b-d).

Conversely, the administration of the TAAR1 agonist RO5166017 (250 nM) to EC slices, did not affect the transient decrease in fEPSPs amplitude induced by OGD (mean relative fEPSP amplitude 65 ± 8% of baseline, $n = 6$, 5 mice $p < 0.001$ *vs* baseline; Fig. 3b), but prevented the long-lasting synaptic depression observed at the end of the reperfusion, mirroring the response to T_1AM (mean relative fEPSP amplitude 100 ± 7% f baseline, n = 6, 5 mice $p > 0.05$ *vs* baseline; $p = 0.029$ *vs* 78 ± 4%, $n = 12$, 9 mice, in vehicle-treated slices; Fig. 3c-d) and suggesting that the T_1AM-TAAR1 system may represent a new pathway able to rescue the ischemia-induced synaptic dysfunction in the EC. Moreover, the concomitant application of T_1AM and RO5166017 mimicked the application of either compound alone, suggesting the involvement of the same mechanism of action (mean relative fEPSP amplitude 100 ± 7% of baseline, $n = 3$, 2 mice $p > 0.05$ *vs* baseline; $p > 0.05$ *vs* 100 ± 7% f baseline, n = 6, 5 mice in RO5166017-treated slices; $p > 0.05$ *vs* 98 ± 5%, n = 8, 5 mice in T_1AM-treated slices; Fig. 3c-d).

3.5. The BDNF-TrkB signalling pathway is involved in T_1AM-mediated neuroprotection

The discovery of TAAR1 involvement in the protective effect of T_1AM raised the important issue of identifying the molecular mediators acting downstream the T_1AM-TAAR1 interaction. In particular, the BDNF-TrkB signalling pathway appeared to us as a suitable candidate given the role of BDNF in synaptic function and plasticity of the EC (Criscuolo et al., 2015), and its modulation by TH (Sui et al., 2010). Interestingly, pre-incubation of slices with anti-TrkB antibody (1 μg/ml) didn't affect the transient decrease in synaptic function immediately following OGD but it prevented the recovery of fEPSPs amplitude at the end of reperfusion; indeed in T_1AM + anti-TrkB-treated slices, the mean relative amplitude of the last 10 min of recording after OGD, was significantly different from that of slices treated with T_1AM alone (63 ± 3%, $n = 7$, 3 mice; $p < 0.001$ *vs* baseline, $p > 0.05$ *vs* 78 ± 4%, $n = 12$, 9 mice, in vehicle-treated slices and $p < 0.001$ *vs* 98 ± 5%, $n = 8$, 5 mice in T_1AM-treated slices; Fig. 4a-e). The same result was observed by either pre-incubating slices with TrkB-IgGs (1 μg/ml), that are able to scavenge the released BDNF in the extracellular medium (mean relative fEPSP amplitude in T_1AM + TrkB-IgG-treated slices was 74 ± 7%, $n = 11$, 6 mice $p < 0.001$ *vs* baseline, $p > 0.05$ *vs* 78 ± 4%, n = 12, 9 mice, in vehicle-treated slices and $p = 0.003$ *vs* 98 ± 5%, $n = 8$, 5 mice, in T_1AM-treated slices; Fig. 4b-e), or by co-perfusing T_1AM with a selective inhibitor of the phosphoinositide-3-kinase (PI3K), LY294002 (10 nM), during the 10 min of OGD (mean fEPSP amplitude in T_1AM + LY294002-treated slices was 59 ± 5%, $n = 7$, 3 mice $p < 0.001$ *vs* baseline, $p > 0.05$ *vs* 78 ± 4%, n = 12, 9 mice, in OGD vehicle treated slices and $p < 0.001$ *vs* 98 ± 5%, n = 8, 5 mice, inT_1AM-treated slices; Fig. 4c-e). Therefore, the absence of a complete rescue of synaptic transmission by T_1AM in presence of either the anti-TrkB antibody or the PI3K inhibitor LY294002 suggests that the activation of the TrkB signalling pathway might be an important molecular event downstream the T_1AM-TAAR1 system. Finally, the lack of effect of T_1AM in presence of TrkB-IgG, able to cage the BDNF released in the extracellular medium, suggests that the cooperation between TAAR1 and TrkB is less likely to occur by a cross-activation of the two receptors, but it is rather due to TAAR1-induced BDNF release in the extracellular medium. In agreement with these results, electrophysiological recordings in EC slices acutely perfused with BDNF (1 ng/ml) during OGD showed a rapid fall in fEPSP amplitude (mean relative fEPSP amplitude 48 ± 5% of baseline, n = 7, 4 mice $p <$ 0.001 *vs* baseline; Fig. 4d) and then a complete recovery at the end of the reperfusion (mean relative fEPSP amplitude was 108 ± 10% of baseline, n = 7, 4 mice, $p < 0.001$ *vs* baseline; $p < 0.001$ *vs* 78 ± 4%, n = 12, 9 mice, in vehicle-treated slices; Fig. 4d-e), demonstrating the protective effect of exogenous application of BDNF. Moreover, the same protective effect was achieved by concomitant administration of T_1AM (5 μM) and BDNF (1 ng/ml), further strengthening the hypothesis of a shared mechanism of action (mean relative fEPSP amplitude 103 ± 7% of baseline, $n = 4$, 2 mice, $p > 0.05$ *vs* 108 ± 10% of baseline, n = 7, 4 mice in BDNF-treated slices; $p > 0.05$ *vs* 98 ± 5%, n = 8, 5 mice in T_1AM-treated slices; Fig. 4d-e). Finally, the involvement of BDNF in T_1AM effect was confirmed by an ELISA BDNF assay performed in EC slices collected after electrophysiology. No significant difference in BDNF protein levels was detected in control slices and slices exposed to OGD (mean BDNF protein concentration relative to total protein levels was 2.81 ± 0.34 pg/mg in control slices, $n = 5$, 2 mice $p > 0.05$ *vs* 3.11 ± 0.78 pg/mg in OGD-treated slices, n = 5, 2 mice; Fig. 4f). However, BDNF levels were higher in slices treated with T_1AM and exposed to OGD compared both to control (mean BDNF protein concentration relative to total protein levels was 5.87 ± 1.04 pg/mg, n = 5, 2 mice, $p <$ 0.05 in OGD + T_1AM-treated slices *vs* 2.81 ± 0.34 pg/mg, n = 5, 2 mice in control slices; Fig. 4f) and OGD-exposed untreated slices (mean BDNF protein concentration relative to total protein levels was 5.87 ± 1.04 pg/mg, n = 5, 2 mice, $p < 0.05$ in OGD + T_1AM-treated slices *vs* 3.11 ± 0.78 pg/mg in OGD-treated slices, n = 5, 2 mice; Fig. 4f), suggesting that T_1AM could protect synaptic function during ischemia by inducing an increase in BDNF production and release. In fact, the co-administration of T_1AM(5 μM) and EPPTB (5 nM) was capable of lowering BDNF protein levels to baseline (mean BDNF protein concentration relative to total protein levels was 3.19 ± 0.35 pg/mg, n = 4, 2 mice $p > 0.05$ in OGD + T1AM + EPPTB-treated slices *vs* 2.81 ± 0.34 pg/mg, n = 5, 2 mice in control slices; Fig. 4f).

3.6. T_1AM-TAAR1 system protects against OGD-induced synaptic dysfunction in a mouse model of AD

Vascular pathologies and AD seem to have some common pathogenic mechanisms. In agreement with this, enhanced vulnerability to ischemia was observed in the EC of a mouse model overexpressing a human form of the APP gene bearing mutations linked to familial AD (mhAPP mice; (Criscuolo et al., 2017). Based on our previous results obtained in C57BL/6 J mice, we investigated whether T_1AM could have a protective effect against OGD-induced synaptic dysfunction in an amyloid-enriched environment. A rapid fall in fEPSP amplitude was observed after the application of OGD in vehicle mhAPP-treated slices (mean relative fEPSP amplitude 40 ± 10% of baseline, $n = 11$, 9 mice $p < 0.001$ *vs* baseline; Fig. 5a) similarly to WT slices. However, mhAPP EC slices showed a significantly enhanced long-term depression at the end of the reperfusion compared to their WT littermates (mean relative fEPSP amplitude was 60 ± 6% of baseline, n = 11, 9 mice $p < 0.001$ *vs* baseline; and $p = 0.025$ *vs* mean ampl. in non-transgenic WT slices that was 78 ± 4%, $n = 12$, 9 mice, Fig. 5a), confirming an increased effect of OGD in an amyloid-enriched environment. Interestingly, the perfusion of T_1AM (5 μM) during OGD did not affect the transient fall in synaptic function induced by OGD (mean relative fEPSP amplitude 58 ± 22% of baseline, $n = 8$, 6 mice $p < 0.001$ *vs* baseline; Fig. 5b) but it was sufficient to prevent the synaptic depression observed in control slices and a complete recovery of fEPSP amplitude was observed at the end of the reperfusion period (mean relative fEPSP amplitude 106 ± 7% of baseline, n = 8, 6 mice $p > 0.05$ *vs* baseline and $p < 0.001$ *vs* 60 ± 6% of baseline, n = 11, 9 mice in mhAPP vehicle-treated slices; Fig. 5b). This finding indicates a protective effect of T_1AM also in the presence of Aβ overproduction. Moreover, we observed that T_1AM protective effect in mhAPP slices was completely abolished by the co-perfusion of EPPTB (5 nM, mean relative fEPSP amplitude in mhAPP +T_1AM + EPPTB was 63 ± 10% of baseline, $n = 6$, 4 mice $p < 0.001$ *vs* 106 ± 7% of baseline, n = 8, 6 mice in mhAPP T_1AM-treated slices; Fig. 5c), similarly to what recorded in WT littermates. As observed in non-transgenic WT EC slices, the administration of EPPTB alone did not affect the long-term synaptic depression induced by ischemia (mean relative fEPSP amplitude in mhAPP + EPPTB slices was 62 ± 7% of baseline, $n = 5$, 2 mice $p < 0.001$

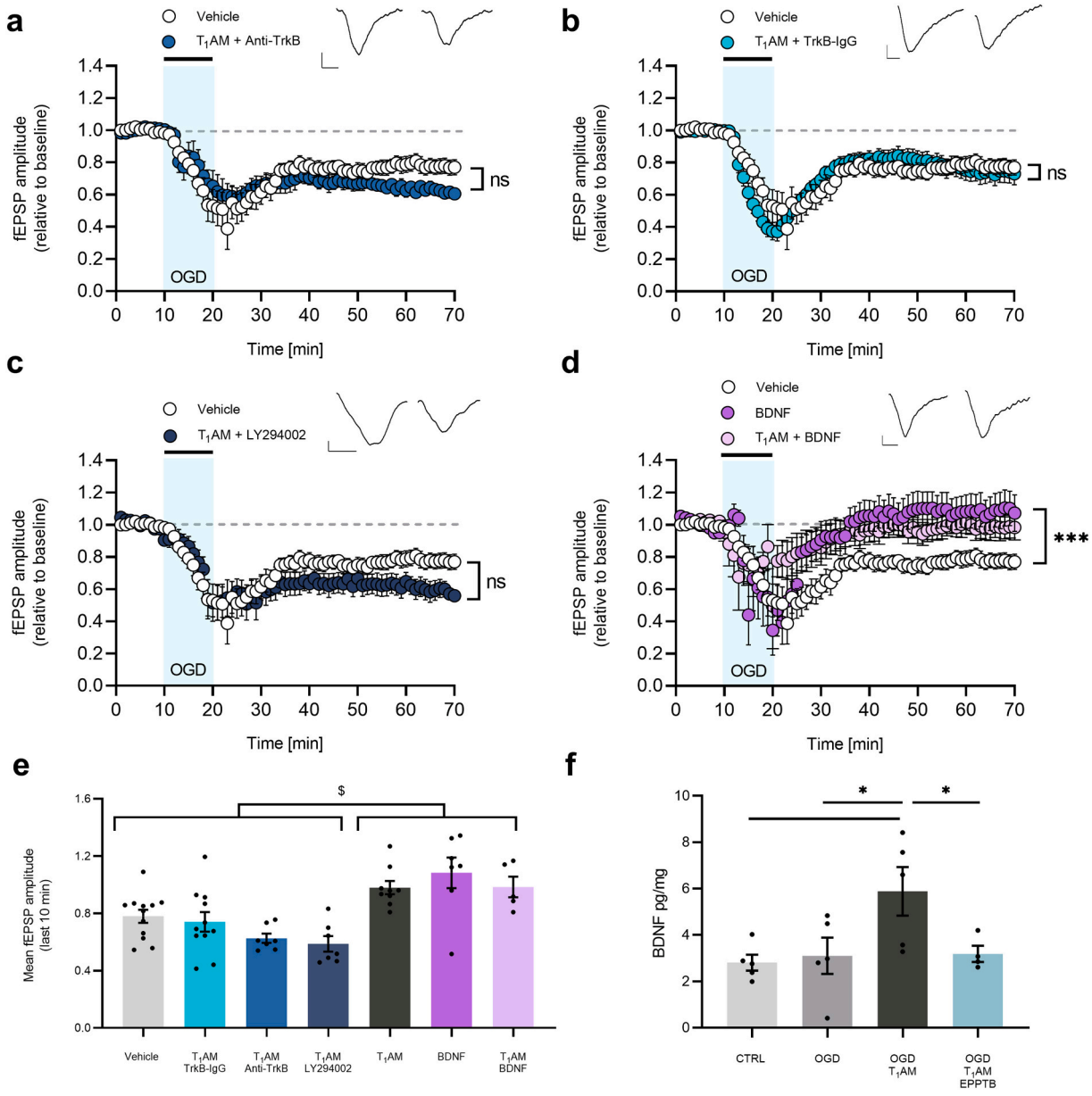

Fig. 4. The BDNF-TrkB signalling pathway is involved in T_1AM-mediated neuroprotection. (a) EC slices perfused with T_1AM (5 μM) and pre-incubated with anti-TrkB antibody (1 μg/ml dark circles) showed a significant decrease in synaptic function following OGD and a long-lasting synaptic depression at the end of the reperfusion not significantly different from that achieved by vehicle-treated slices (white circles). (b) EC slices perfused with T_1AM (5 μM) and pre-incubated with TrkB-IgG (1 μg/ml, dark circles) showed a significant decrease in synaptic function following OGD and a long-lasting synaptic depression at the end of the reperfusion not significantly different from that of vehicle-treated slices (white circles). (c) EC slices co-perfused with T_1AM (5 μM) + the PI3K inhibitor LY294002 (10 nM, dark circles) showed a significant decrease in synaptic function following OGD and a long-lasting synaptic depression at the end of the reperfusion not significantly different from vehicle-treated slices (white circles). (d) EC slices treated with BDNF (1 ng/ml, dark circles) showed a significant decrease in synaptic amplitude following OGD but a complete rescue of synaptic function at the end of the reperfusion. The mean relative fEPSP amplitude reached by BDNF-treated slices at the end of the reperfusion was significantly different from vehicle-treated slices (white circles). The same result was observed in T_1AM (5 μM) + BDNF(1 ng/ml)-treated slices (light circles). The shaded areas on (a to d) plots indicate the application time of OGD and the dark bars indicate the timeline of drugs application. Inserts in (a to d) show typical traces of fEPSP recordings during the baseline and at the end of the reperfusion (scale bar vert. = 0.2 mV, hor. = 2 ms). Error bars indicate SEM. Two-way ANOVA repeated measures and Holm-Sidak method for post-hoc multiple comparisons, ns = not significant, $^{***}p < 0.001$. (e) Summary histogram showing all significant pairwise multiple comparisons between groups (two-way ANOVA RM, post-hoc Holm-Sidak method, $ = significant comparisons). Mean fEPSP at the end of the reperfusion was 78 ± 4% of baseline in vehicle-treated slices $p < 0.001$ *vs* 108 ± 10% of baseline in BDNF-treated slices, $p = 0.029$ *vs* 100 ± 7% of baseline in T_1AM + RO5166017-treated slices, $p = 0.024$ *vs* 98 ± 5% of baseline in T_1AM-treated slices; mean fEPSP 74 ± 7% of baseline in T_1AM + TrkB-IgG-treated slices $p < 0.001$ *vs* BDNF-treated slices, $p = 0.004$ *vs* T_1AM + RO5166017-treated slices, $p = 0.003$ *vs* T_1AM-treated slices; mean fEPSP 63 ± 3% in T_1AM + anti-TrkB-treated slices $p < 0.001$ *vs* BDNF-treated slices, T_1AM + RO5166017-treated slices and T_1AM-treated slices; mean fEPSP 59 ± 5% of baseline in T_1AM + LY294002-treated slices $p < 0.001$ *vs* BDNF-treated slices, T_1AM + RO5166017-treated slices and T_1AM-treated slices. (f) The plot represents averaged BDNF levels measured using ELISA and expressed as pg of BDNF/mg of total proteins. One-way ANOVA and Holm-Sidak method for post-hoc multiple comparisons, ns = not significant, $^{*}p < 0.05$. Error bars indicate SEM.

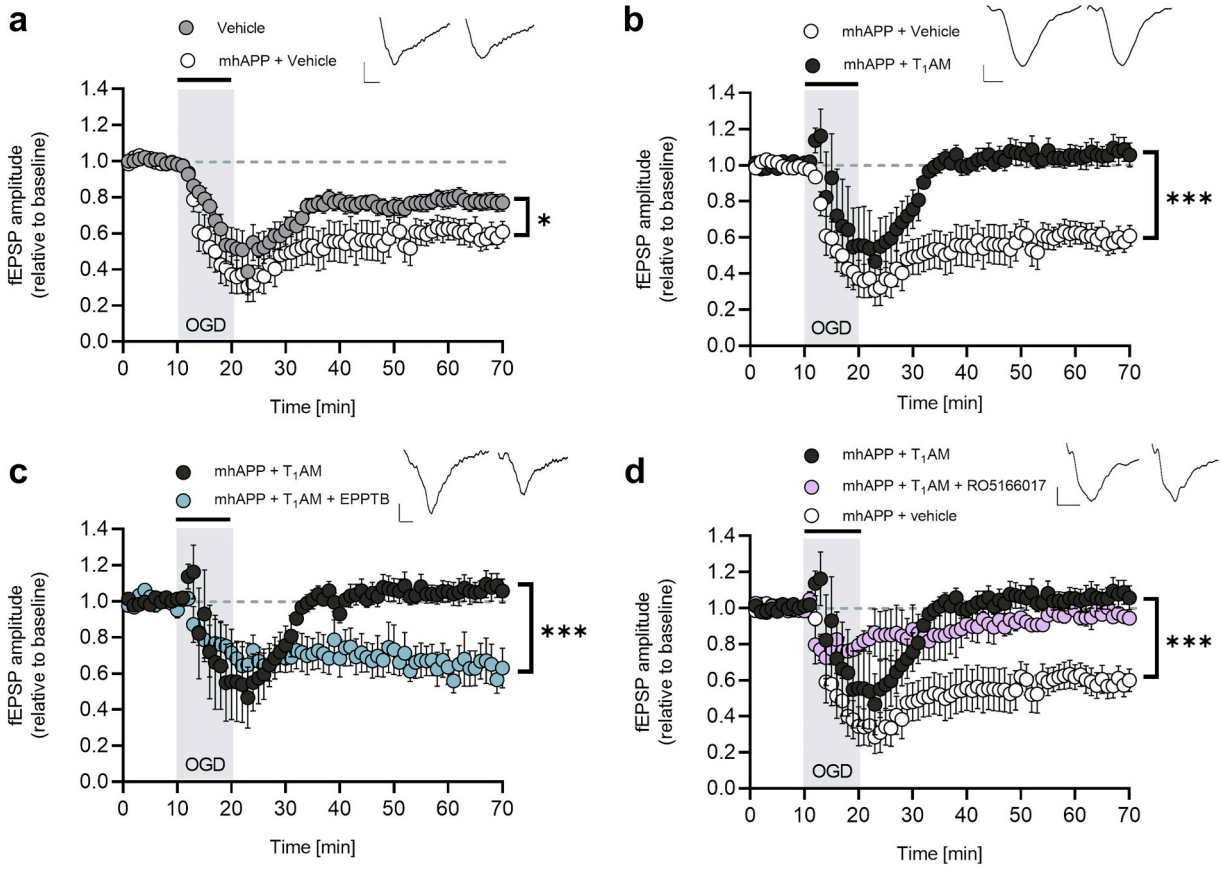

Fig. 5. T_1AM-TAAR1 system protects against OGD-induced synaptic dysfunction in a mouse model of AD. (a) Transgenic mhAPP EC slices treated with vehicle (white circles) showed a significantly enhanced synaptic depression following OGD compared to non-transgenic WT EC slices (dark circles). (b) Transgenic mhAPP EC slices perfused with T_1AM (5 μM, dark circles) showed a significant recovery in synaptic function following OGD compared to mhAPP +vehicle-treated slices (white circles). (c) Transgenic mhAPP EC slices co-perfused with T_1AM (5 μM) and EPPTB (5 nM) showed a significant long-term depression following OGD compared to mhAPP + T;AM-treated slices (dark circles). (d) Transgenic mhAPP EC slices perfused with RO5166017 (250 nM, dark circles) showed a significant recovery in synaptic function following OGD compared to mhAPP + vehicle-treated slices (white circles). The same effect was observed following concomitant application of T_1AM and RO5166017 (light circles). The shaded areas on (a to d) plots indicate the application time of OGD and the dark bars indicate the timeline of drugs application. Inserts in (a to d) show typical traces of fEPSP recordings during the baseline and at the end of the reperfusion (vert scale bar = 0.2 mV; horiz. Scale bar = 2 ms). Error bars indicate SEM. Two-way ANOVA repeated measures and Holm-Sidak method for post-hoc multiple comparisons, ns = not significant, $*p < 0.05$, $***p < 0.001$.

vs baseline and $p > 0.05$ *vs* 60 ± 6% of baseline, $n = 11$, 9 mice in mhAPP vehicle-treated slices; Fig. 6c). In contrast a protection was achieved by the administration of the selective TAAR1 agonist (mean relative fEPSP amplitude in mhAPP + RO5166017 was 106 ± 9% of baseline, $n = 7$, 5 mice $p > 0.05$ *vs* baseline and $p < 0.001$ *vs* 60 ± 6% of baseline, $n = 11$, 9 mice, in vehicle+mhAPP slices; Fig. 5d). Moreover, the concomitant application of T_1AM and RO5166017 had a similar protective effect, confirming the involvement of TAAR1 in T_1AM mechanism of action (mean relative fEPSP amplitude 92 in mhAPP + T1AM + RO5166017 slices was 92 ± 5% of baseline, $n = 3$, 2 mice $p > 0.05$ *vs* 106 ± 7% of baseline, $n = 8$, 6 mice in mhAPP T_1AM-treated slices; $p > 0.05$ *vs* 106 ± 9% of baseline, $n = 7$, 5 mice in mhAPP+RO5166017-treated slices; Figs. 5d-6c).

3.7. The BDNF-TrkB signalling pathway is involved in T_1AM-mediated neuroprotection in an amyloid-enriched environment

To confirm the involvement of the BDNF-TrkB signalling pathway in an amyloid-enriched environment, we repeated key electrophysiological experiments in slices obtained from mhAPP mice. In agreement with the results obtained in WT slices, the co-perfusion of T_1AM (5 μM) and the selective PI3K-inhibitor LY294002 (10 nM) was sufficient to abolish T_1AM protective effect against synaptic dysfunction in mhAPP EC slices (mean relative fEPSP amplitude in mhAPP + T_1AM + LY294002 was 71 ± 8% of baseline, n = 5, 3 mice $p < 0.001$ *vs* baseline, $p > 0.05$ *vs* 60 ± 6% of baseline, n = 11, 9 mice, in mhAPP+vehicle-treated slices and $p < 0.001$ *vs* 106 ± 7% of baseline, n = 8, 6 mice in mhAPP T_1AM-treated slices; Fig. 6a-c), demonstrating the involvement of the main TrKB-mediated signalling pathway. Moreover, exogenous application of BDNF (1 ng/ml) completely prevented the long-term synaptic failure observed in mhAPP + vehicle slices (mean relative fEPSP amplitude was 103 ± 7% of baseline, n = 7, 3 mice $p < 0.001$ *vs* 60 ± 6% of baseline, n = 11, 9 mice, in mhAPP+vehicle-treated slices; Fig. 6b-c), as observed in non-transgenic WT EC slices, proving the protective effect of BDNF against ischemia-induced synaptic dysfunction in an amyloid-enriched environment. In addition, T_1AM and BDNF protective effects seem to occlude each other (mean relative fEPSP amplitude 109 ± 8% of baseline, $n = 4$, 2 mice $p > 0.05$ *vs* 106 ± 7% of baseline, n = 8, 6 mice in mhAPP+T_1AM-treated slices; $p > 0.05$ *vs* 103 ± 7% of baseline, n = 7, 3 mice in mhAPP+BDNF-treated slices; Fig. 6b-c), supporting the hypothesis of a common mechanism of action as seen for WT slices. Moreover,the ELISA assay showed significantly higher levels of BDNF protein in mhAPP EC slices not exposed OGD compared to mhAPP EC slices exposed to transient ischemia (mean BDNF level was 11 ± 2 pg/mg of total protein in control mhAPP EC slices, n = 4, 2 mice $p < 0.05$ *vs* 3 ± 1 pg/mg of total protein, n = 4, 2 mice in OGD-treated mhAPP EC

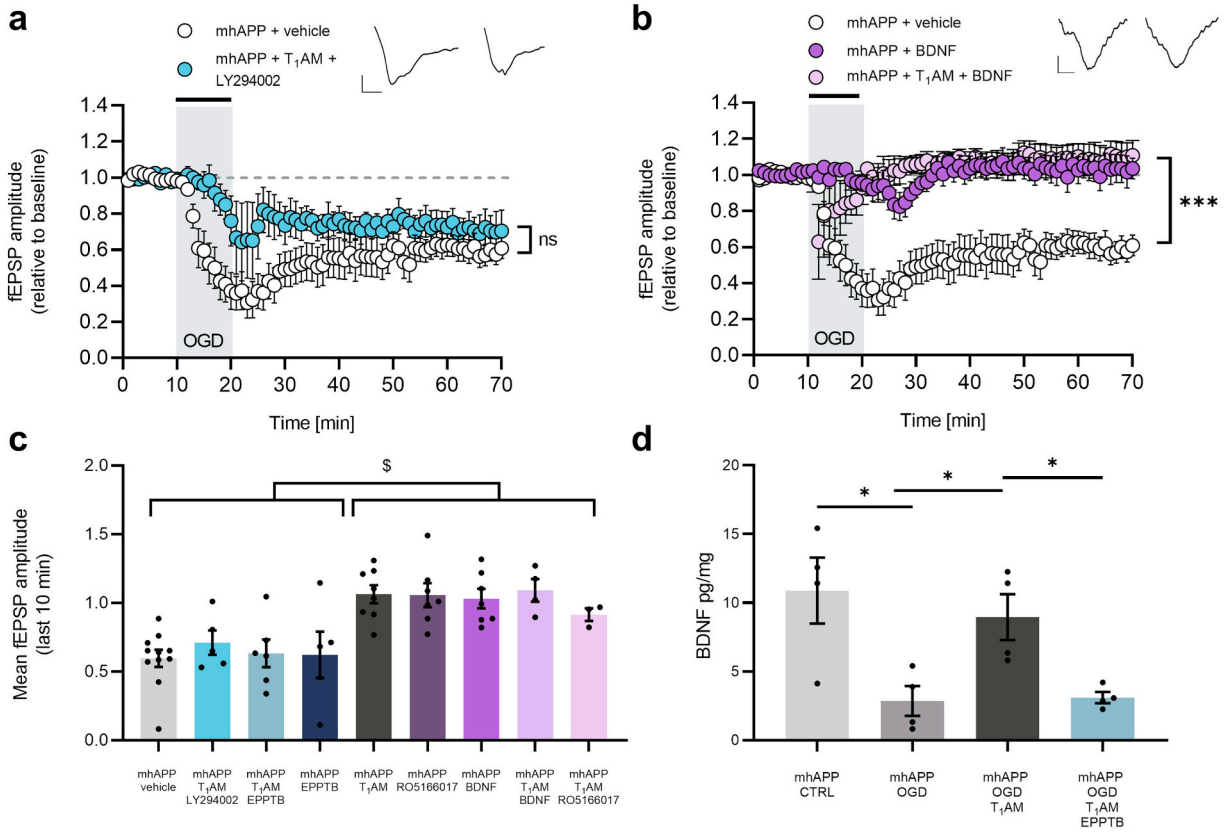

Fig. 6. The BDNF-TrkB signalling pathway is involved in T_1AM-mediated neuroprotection in an amyloid-enriched environment. (a) Transgenic mhAPP EC slices co-perfused with T_1AM (5 μM) and LY294002 (10 nM,dark circles) showed a rapid fall in fEPSP amplitude following ischemia and a long-term synaptic depression similar to that achieved by mhAPP + vehicle-treated slices (white circles). (b) EC mhAPP slices treated with BDNF (1 ng/ml, dark circles) showed a complete recovery of fEPSP amplitude at the end of the reperfusion, reaching a mean relative fEPSP amplitude significantly different from that achieved by mhAPP + vehicle-treated slices (white circles). The shaded areas on (a,b) plots indicate the application time of OGD and the dark bars indicate the timeline of drugs application. Inserts in (a,b) show typical traces of fEPSP recordings during the baseline and at the end of the reperfusion(scale bar vert. = 0.2 mV, hor. = 2 ms). Error bars indicate SEM. Two-way ANOVA repeated measures and Holm-Sidak method for post-hoc multiple comparisons, ns = not significant, ***$p < 0.001$. (c) Summary histogram showing all significant pairwise multiple comparisons between groups (two-way ANOVA RM, post-hoc Holm-Sidak method, $ significant comparisons). Mean fEPSP at the end of the reperfusion was 60 ± 6% of baseline in mhAPP+vehicle-treated slices $p < 0.001$ *vs* 103 ± 7% of baseline in mhAPP+BDNF-treated slices, $p < 0.001$ *vs* 106 ± 9% of baseline in mhAPP+RO5166017-treated slices, $p < 0.001$ *vs* 106 ± 7% in mhAPP+T_1AM-treated slices, $p < 0.001$ *vs* 109 ± 8% in mhAPP+T_1AM + RO5166017; mean fEPSP 63 ± 10% of baseline in mhAPP+T_1AM + EPPTB-treated slices $p < 0.001$ *vs* mhAPP+BDNF-treated slices, mhAPP+RO5166017-treated slices and mhAPP+T_1AM-treated slices, $p < 0.001$ *vs* mhAPP+T_1AM + RO5166017; mean fEPSP 62 ± 17% of baseline in mhAPP+EPPTB-treated slices $p < 0.001$ *vs* mhAPP+BDNF-treated slices, mhAPP+RO5166017-treated slices and mhAPP+T_1AM-treated slices, $p < 0.001$ *vs* mhAPP+T_1AM + RO5166017; mean fEPSP 71 ± 8% of baseline in mhAPP+T_1AM + LY294002-treated slices $p < 0.01$ *vs* mhAPP+BDNF-treated slices, mhAPP+RO5166017-treated slices and $p < 0.001$ *vs* mhAPP+T_1AM-treated slices and mhAPP+T_1AM + RO5166017. (d) The plot represents averaged BDNF levels measured using ELISA and expressed as pg of BDNF/mg of total proteins. Error bars indicate SEM. Two-way ANOVA repeated measures and Holm-Sidak method for post-hoc multiple comparisons, ns = not significant, *$p < 0.05$).

slices; Fig. 6d). However, the administration of T_1AM (5 μM) was capable of restoring BDNF protein levels following OGD (mean BDNF protein level was 8.96 ± 2.4 pg/mg of protein, n = 4, 2 mice $p > 0.05$ in OGD + T_1AM-treated mhAPP slices *vs* 11 ± 2 pg/mg in control mhAPP EC slices, n = 4, 2 mice; Fig. 6d). Moreover, as observed in non-transgenic WT slices, the co-administration of T_1AM (5 μM) and EPPTB (5 nM) during OGD completely prevented the increase in BDNF protein levels observed in slices treated with T_1AM alone (mean BDNF protein level was 3.10 ± 0.41 pg/mg, n = 4, 2 mice $p < 0.05$ *vs* 8.96 ± 2.4 pg/mg, n = 4, 2 mice $p > 0.05$ in OGD + T1AM-treated mhAPP slices; Fig. 6d), suggesting that TAAR1 activation is a crucial step in the response to T_1AM.

4. Discussion

Transient ischemia has been demonstrated to increase the expression of key proteins usually linked to AD, such as the β-amyloid peptide, and to favour their accumulation in the brain (Abe et al., 1991; Uryu et al., 2002; Yokota et al., 1996). Indeed, hypoxia can function as a trigger for Aβ-dependent synaptic impairment in the EC and an increased vulnerability to ischemic damage has been observed in an amyloid-enriched environment (Origlia et al., 2014), suggesting that ischemia and AD could act in synergy in promoting dementia and raising the important issue of identifying key molecular targets that can be manipulated to counteract the cognitive decline. Thyroid hormones and their metabolites may represent a link between ischemia and AD, as it is well known that hypothyroidism can increase the risk for stroke (Bai et al., 2014; Gao et al., 2013; Iwen et al., 2013), and it is a recognized cause of cognitive impairment (Cummings et al., 1980; Smith and Kiloh, 1981). In particular, we investigated the role of a novel endogenous TH metabolite, T_1AM, widely distributed in mouse tissues (Chiellini et al., 2007; Saba et al., 2010; Scanlan, 2009; Scanlan et al., 2004; Zucchi et al., 2014).

Using an *in vitro* model of transient ischemia, we observed that exogenous T_1AM can positively affect the functional outcome of the EC after an ischemic episode. In fact, EC slices treated with T_1AM during

OGD completely recovered the fEPSPs amplitude at the end of the reperfusion. Since previous works have reported that some effects elicited after the administration of exogenous T_1AM are due to its main oxidative metabolite (Laurino et al., 2018; Laurino et al., 2015; Musilli et al., 2014), we investigated the effect of TA_1 on OGD, but obtained negative results. The putative T_1AM precursor T_3 was also ineffective. These findings are in agreement with our previous report in which TA_1 and T_3 were not effective in ameliorating EC synaptic dysfunction induced by exogenous administration of Aβ, confirming the specific protective effect of T_1AM.

T_1AM concentration in the effluent, assumed to be in equilibrium with the extracellular space, varies following its administration and washout phases, though always remaining 5 to 50-fold lower than the administered dose. In parallel, a release of TA_1, and no other metabolites, could be detected. This indicates that exogenous T_1AM is rapidly taken up and deaminated to TA_1, which is then released into the extracellular space. Furthermore, OGD led to minimum but significant TA_1 release also in absence of exogenous T_1AM. It remains to be determined whether TA_1 is produced by oxidative deamination of endogenous T1AM, and whether this phenomenon should be considered as a deleterious effect of ischemia or rather as a protective event.

Regarding the mechanism of action, T_1AM does not bind the nuclear thyroid hormone receptors (TRs) but it stimulates with nanomolar affinity TAAR1, a G protein-coupled receptor. Additional targets are represented by apolipoprotein B100 (Roy et al., 2012), alpha-2A adrenergic receptors (ADRA2A; (Regard et al., 2007), mitochondrial ATP synthase (Cumero et al., 2012), and membrane monoamine transporters (Snead et al., 2007), but the functional relevance of these interactions is still not completely clear. We focused on TAAR1 since we had previously demonstrated that the T_1AM-TAAR1 signalling pathway has a protective effect on synaptic plasticity in the mouse EC in the presence of the beta-amyloid peptide (Accorroni et al., 2019). Using a pharmacological approach, we demonstrated that inhibition of TAAR1 was sufficient to prevent T_1AM protective effect on synaptic function, and conversely the stimulation of TAAR1 in the absence of T_1AM was sufficient to obtain a complete recovery of the synaptic transmission, as observed in T_1AM-treated slices.

Looking to downstream targets of the T_1AM-TAAR1 axis, we hypothesized a possible role for BDNF and its receptor TrkB. This hypothesis is based on the evidence that BDNF plays an incontrovertible role on synaptic plasticity, reduces OGD–induced damage in brain slices (González-Rodríguez et al., 2019; Tecuatl et al., 2018) and protects EC synapses from Aβ injury (Criscuolo et al., 2015). Notably, BDNF can be modulated by TH levels (Sui et al., 2010) and T_1AM was shown to act on PI3K, a kinase acting downstream TrkB activation (Bellusci et al., 2017). Our hypothesis is also supported by a recent work in hypothyroid rats, showing learning and memory impairment that were associated with oxidative stress and reduced levels of BDNF. Interestingly, increasing BDNF levels in hypothyroid rats was capable of improving behaviour and brain tissue damage (Memarpour et al., 2020).

To test our hypothesis, we first blocked BDNF signalling during T_1AM administration either by a pre-incubation of EC slices with an anti-TrkB antibody or by the administration of a PI3K selective inhibitor, LY294002. Our results clearly show that inhibition of BDNF action on TrKB reduces the protective activity of T_1AM. This is consistent with the hypothesis that recovery of synaptic transmission after OGD is induced by BDNF *per se*, as observed in a previous report in hippocampal slices (Tecuatl et al., 2018). The role of BDNF in T_1AM-induced neuroprotection was confirmed by the increased BDNF levels observed in T_1AM treated slices, an effect which was abolished by co-perfusion with the TAAR1 selective antagonist EPPTB.

We have previously reported that ischemia-induced synaptic depression in the EC is enhanced in an amyloid-enriched environment, due to increased Aβ levels induced by OGD (Origlia et al., 2014). To investigate whether T_1AM protective effect was preserved in an AD model, we exposed EC slices obtained from mhAPP mice to the OGD protocol. The vulnerability to ischemia was enhanced in AD mice, as expected, the acute administration of T_1AM completely prevented the long-term synaptic depression observed in vehicle-treated mhAPP slices, and TAAR1 involvement was confirmed. In mhAPP slices BDNF levels were increased by T_1AM, similarly to what observed in WT slices.

Interestingly, the basal levels of BDNF, measured in the absence OGD, were higher in mhAPP respect to WT animals. This may be related to the hyperexcitability observed in mhAPP mice (Harris et al., 2010), since the EC is an area classically known to be prone to epileptic–like activity (Lindvall et al., 1994) and there is evidence that BDNF overexpression can lead to spontaneous seizures (Croll et al., 1999). However, it has to be noticed thata protective effect, mediated by BDNF, was induced by systemic administration of TH in rats exposed to Aβ-damage (Shabani et al., 2018). Moreover, in mhAPP slices the administration of BDNF during OGD was capable of preventing ischemia-induced synaptic dysfunction, suggesting that BDNF could have a protective role against AD neurodegeneration. In agreement with this hypothesis, decreased serum BDNF levels have been found in AD patients (Ng et al., 2019) and it is possible that brain ischemia could contribute in decreasing BDNF levels, thus accelerating the development of cognitive impairment. In this scenario, Aβ and ischemia would be synergic in promoting cognitive dysfunction, and the possibility to regulate a molecular pathway capable of preserving synaptic function in areas crucially involved in the development of the disease would have potential therapeutic implications. Since T1AM and synthetic analogues were shown to be effective in ameliorating neurodegeneration (Accorroni et al., 2019; Bellusci et al., 2020; Bellusci et al., 2017), these compounds and other TAAR1 agonists may represent a novel strategy for neuroprotection.

In summary, we showed that the T_1AM-TAAR1 signalling pathway is able to protect against ischemia-induced synaptic dysfunction either in WT or in an amyloid-enriched environment and that TAAR1 stimulation can increase BDNF protein levels in EC slices. It should however be acknowledged that all our experiments were performed using *in vitro* models of disease. Further investigations will be necessary to confirm the present findings and to evaluate whether they can be reproduced *in vivo*.

Acknowledgements

The authors gratefully acknowledge R. Di Renzo for technical assistance, Dr. F. Biondi for the excellent animal care. This work was supported by CNR research program.

References

Abe, K., Tanzi, R.E., Kogure, K., 1991. Selective induction of Kunitz-type protease inhibitor domain-containing amyloid precursor protein mRNA after persistent focal ischemia in rat cerebral cortex. Neurosci. Lett. 125, 172–174.

Accorroni, A., Giorgi, F.S., Donzelli, R., Lorenzini, L., Prontera, C., Saba, A., Vergallo, A., Tognoni, G., Siciliano, G., Baldacci, F., Bonuccelli, U., Clerico, A., Zucchi, R., 2017. Thyroid hormone levels in the cerebrospinal fluid correlate with disease severity in euthyroid patients with Alzheimer's disease. Endocrine 55, 981–984.

Accorroni, A., Rutigliano, G., Sabatini, M., Frascarelli, S., Borsò, M., Novelli, E., Bandini, L., Ghelardoni, S., Saba, A., Zucchi, R., Origlia, N., 2019. Exogenous 3-Iodothyronamine rescues the entorhinal cortex from β-amyloid toxicity. Thyroid. https://doi.org/10.1089/thy.2019.0255.

Bai, M.-F., Gao, C.-Y., Yang, C.-K., Wang, X.-P., Liu, J., Qi, D.-T., Zhang, Y., Hao, P.-Y., Li, M.-W., 2014. Effects of thyroid dysfunction on the severity of coronary artery lesions and its prognosis. J. Cardiol. 64, 496–500.

Belakavadi, M., Dell, J., Grover, G.J., Fondell, J.D., 2011. Thyroid hormone suppression of β-amyloid precursor protein gene expression in the brain involves multiple epigenetic regulatory events. Mol. Cell. Endocrinol. 339, 72–80.

Bellusci, L., Laurino, A., Sabatini, M., Sestito, S., Lenzi, P., Raimondi, L., Rapposelli, S., Biagioni, F., Fornai, F., Salvetti, A., Rossi, L., Zucchi, R., Chiellini, G., 2017. New insights into the potential roles of 3-Iodothyronamine (T1AM) and newly developed Thyronamine-like TAAR1 agonists in neuroprotection. Front. Pharmacol. 8, 905.

Bellusci, L., Runfola, M., Carnicelli, V., Sestito, S., Fulceri, F., Santucci, F., Lenzi, P., Fornai, F., Rapposelli, S., Origlia, N., Zucchi, R., Chiellini, G., 2020. Endogenous 3-Iodothyronamine (T1AM) and synthetic thyronamine-like analog SG-2 act as novel pleiotropic neuroprotective agents through the modulation of SIRT6. Molecules 25. https://doi.org/10.3390/molecules25051054.

Braak, H., Braak, E., 1995. Staging of Alzheimer's disease-related neurofibrillary changes. Neurobiol. Aging 16, 271–278 (discussion 278–84).
Chiellini, G., Frascarelli, S., Ghelardoni, S., Carnicelli, V., Tobias, S.C., DeBarber, A., Brogioni, S., Ronca-Testoni, S., Cerbai, E., Grandy, D.K., Scanlan, T.S., Zucchi, R., 2007. Cardiac effects of 3-iodothyronamine: a new aminergic system modulating cardiac function. FASEB J. 21, 1597–1608.
Criscuolo, C., Fabiani, C., Bonadonna, C., Origlia, N., Domenici, L., 2015. BDNF prevents amyloid-dependent impairment of LTP in the entorhinal cortex by attenuating p38 MAPK phosphorylation. Neurobiol. Aging 36, 1303–1309.
Criscuolo, C., Fontebasso, V., Middei, S., Stazi, M., Ammassari-Teule, M., Yan, S.S., Origlia, N., 2017. Entorhinal cortex dysfunction can be rescued by inhibition of microglial RAGE in an Alzheimer's disease mouse model. Sci. Rep. 7, 42370.
Croll, S.D., Suri, C., Compton, D.L., Simmons, M.V., Yancopoulos, G.D., Lindsay, R.M., Wiegand, S.J., Rudge, J.S., Scharfman, H.E., 1999. Brain-derived neurotrophic factor transgenic mice exhibit passive avoidance deficits, increased seizure severity and in vitro hyperexcitability in the hippocampus and entorhinal cortex. Neuroscience 93, 1491–1506.
Cumero, S., Fogolari, F., Domenis, R., Zucchi, R., Mavelli, I., Contessi, S., 2012. Mitochondrial F(0) F(1) -ATP synthase is a molecular target of 3-iodothyronamine, an endogenous metabolite of thyroid hormone. Br. J. Pharmacol. 166, 2331–2347.
Cummings, J., Frank Benson, D., LoVerme, S., 1980. Reversible dementia: illustrative cases, definition, and review. JAMA 243, 2434–2439.
Farbood, Y., Shabani, S., Sarkaki, A., Mard, S.A., Ahangarpour, A., Khorsandi, L., 2017. Peripheral and central administration of T3 improved the histological changes, memory and the dentate gyrus electrophysiological activity in an animal model of Alzheimer's disease. Metab. Brain Dis. 32, 693–701.
Frascarelli, S., Ghelardoni, S., Chiellini, G., Galli, E., Ronca, F., Scanlan, T.S., Zucchi, R., 2011. Cardioprotective effect of 3-iodothyronamine in perfused rat heart subjected to ischemia and reperfusion. Cardiovasc. Drugs Ther. 25, 307–313.
Ganguli, M., Burmeister, L.A., Seaberg, E.C., Belle, S., DeKosky, S.T., 1996. Association between dementia and elevated TSH: a community-based study. Biol. Psychiatry 40, 714–725.
Gao, N., Zhang, W., Zhang, Y.-Z., Yang, Q., Chen, S.-H., 2013. Carotid intima-media thickness in patients with subclinical hypothyroidism: a meta-analysis. Atherosclerosis 227, 18–25.
Girouard, H., Iadecola, C., 2006. Neurovascular coupling in the normal brain and in hypertension, stroke, and Alzheimer disease. J. Appl. Physiol. 100, 328–335.
González-Rodríguez, P., Ugidos, I.F., Pérez-Rodríguez, D., Anuncibay-Soto, B., Santos-Galdiano, M., Font-Belmonte, E., Gonzalo-Orden, J.M., Fernández-López, A., 2019. Brain-derived neurotrophic factor alleviates the oxidative stress induced by oxygen and glucose deprivation in an ex vivo brain slice model. J. Cell. Physiol. 234, 9592–9604.
Harris, J.A., Devidze, N., Verret, L., Ho, K., Halabisky, B., Thwin, M.T., Kim, D., Hamto, P., Lo, I., Yu, G.-Q., Palop, J.J., Masliah, E., Mucke, L., 2010. Transsynaptic progression of amyloid-β-induced neuronal dysfunction within the entorhinal-hippocampal network. Neuron 68, 428–441.
Hoefig, C.S., Wuensch, T., Rijntjes, E., Lehmphul, I., Daniel, H., Schweizer, U., Mittag, J., Köhrle, J., 2015. Biosynthesis of 3-Iodothyronamine from T4 in murine intestinal tissue. Endocrinology 156, 4356–4364.
Hoefig, C.S., Zucchi, R., Köhrle, J., 2016. Thyronamines and derivatives: physiological relevance, pharmacological actions, and future research directions. Thyroid 26, 1656–1673.
Iwen, K.A., Schröder, E., Brabant, G., 2013. Thyroid hormones and the metabolic syndrome. Eur. Thyroid. J. 2, 83–92.
Johansson, P., Almqvist, E.G., Johansson, J.-O., Mattsson, N., Hansson, O., Wallin, A., Blennow, K., Zetterberg, H., Svensson, J., 2013. Reduced cerebrospinal fluid level of thyroxine in patients with Alzheimer's disease. Psychoneuroendocrinology 38, 1058–1066.
Köhrle, J., Biebermann, H., 2019. 3-Iodothyronamine-a thyroid hormone metabolite with distinct target profiles and mode of action. Endocr. Rev. 40, 602–630.
Köhrle, J., Lehmphul, I., Pietzner, M., Renko, K., Rijntjes, E., Richards, K., Anselmo, J., Danielsen, M., Jonklaas, J., 2019. 3,5-T2-a Janus-faced thyroid hormone metabolite exerts both canonical T3-mimetic endocrine and Intracrine hepatic action. Front. Endocrinol. 10, 787.
Landucci, E., Gencarelli, M., Mazzantini, C., Laurino, A., Pellegrini-Giampietro, D.E., Raimondi, L., 2019. N-(3-Ethoxy-phenyl)-4-pyrrolidin-1-yl-3-trifluoromethyl-benzamide (EPPTB) prevents 3-iodothyronamine (T1AM)-induced neuroprotection against kainic acid toxicity. Neurochem. Int. 129, 104460.
Laurino, A., De Siena, G., Saba, A., Chiellini, G., Landucci, E., Zucchi, R., Raimondi, L., 2015. In the brain of mice, 3-iodothyronamine (T1AM) is converted into 3-iodo-thyroacetic acid (TA1) and it is included within the signaling network connecting thyroid hormone metabolites with histamine. Eur. J. Pharmacol. 761, 130–134.
Laurino, A., Landucci, E., Raimondi, L., 2018. Central effects of 3-Iodothyronamine reveal a novel role for mitochondrial monoamine oxidases. Front. Endocrinol. 9, 290.
Lindvall, O., Kokaia, Z., Bengzon, J., Elmér, E., Kokaia, M., 1994. Neurotrophins and brain insults. Trends Neurosci. 17, 490–496.
Losi, G., Garzon, G., Puia, G., 2008. Nongenomic regulation of glutamatergic neurotransmission in hippocampus by thyroid hormones. Neuroscience 151, 155–163.
Manni, M.E., De Siena, G., Saba, A., Marchini, M., Landucci, E., Gerace, E., Zazzeri, M., Musilli, C., Pellegrini-Giampietro, D., Matucci, R., Zucchi, R., Raimondi, L., 2013. Pharmacological effects of 3-iodothyronamine (T1AM) in mice include facilitation of memory acquisition and retention and reduction of pain threshold. Br. J. Pharmacol. 168, 354–362.
Memarpour, S., Beheshti, F., Baghcheghi, Y., Vafaei, A.A., Hosseini, M., Rashidy-Pour, A., 2020. Neuronal nitric oxide inhibitor 7-Nitroindazole improved brain-derived neurotrophic factor and attenuated brain tissues oxidative damage and learning and memory impairments of hypothyroid juvenile rats. Neurochem. Res. 45, 2775–2785.
Mucke, L., Masliah, E., Yu, G.Q., Mallory, M., Rockenstein, E.M., Tatsuno, G., Hu, K., Kholodenko, D., Johnson-Wood, K., McConlogue, L., 2000. High-level neuronal expression of abeta 1-42 in wild-type human amyloid protein precursor transgenic mice: synaptotoxicity without plaque formation. J. Neurosci. 20, 4050–4058.
Musilli, C., De Siena, G., Manni, M.E., Logli, A., Landucci, E., Zucchi, R., Saba, A., Donzelli, R., Passani, M.B., Provensi, G., Raimondi, L., 2014. Histamine mediates behavioural and metabolic effects of 3-iodothyroacetic acid, an endogenous end product of thyroid hormone metabolism. Br. J. Pharmacol. 171, 3476–3484.
Ng, T.K.S., Ho, C.S.H., Tam, W.W.S., Kua, E.H., Ho, R.C.-M., 2019. Decreased serum brain-derived neurotrophic factor (BDNF) levels in patients with Alzheimer's disease (AD): a systematic review and meta-analysis. Int. J. Mol. Sci. 20 https://doi.org/10.3390/ijms20020257.
O'Barr, S.A., Oh, J.S., Ma, C., Brent, G.A., Schultz, J.J., 2006. Thyroid hormone regulates endogenous amyloid-beta precursor protein gene expression and processing in both in vitro and in vivo models. Thyroid 16, 1207–1213.
Origlia, N., Righi, M., Capsoni, S., Cattaneo, A., Fang, F., Stern, D.M., Chen, J.X., Schmidt, A.M., Arancio, O., Yan, S.D., Domenici, L., 2008. Receptor for advanced glycation end product-dependent activation of p38 mitogen-activated protein kinase contributes to amyloid-beta-mediated cortical synaptic dysfunction. J. Neurosci. 28, 3521–3530.
Origlia, N., Capsoni, S., Cattaneo, A., Fang, F., Arancio, O., Yan, S.D., Domenici, L., 2009. Abeta-dependent inhibition of LTP in different intracortical circuits of the visual cortex: the role of RAGE. J. Alzheimers Dis. 17, 59–68.
Origlia, N., Bonadonna, C., Rosellini, A., Leznik, E., Arancio, O., Yan, S.S., Domenici, L., 2010. Microglial receptor for advanced glycation end product-dependent signal pathway drives beta-amyloid-induced synaptic depression and long-term depression impairment in entorhinal cortex. J. Neurosci. 30, 11414–11425.
Origlia, N., Criscuolo, C., Arancio, O., Yan, S.S., Domenici, L., 2014. RAGE inhibition in microglia prevents ischemia-dependent synaptic dysfunction in an amyloid-enriched environment. J. Neurosci. 34, 8749–8760.
Regard, J.B., Kataoka, H., Cano, D.A., Camerer, E., Yin, L., Zheng, Y.-W., Scanlan, T.S., Hebrok, M., Coughlin, S.R., 2007. Probing cell type-specific functions of Gi in vivo identifies GPCR regulators of insulin secretion. J. Clin. Invest. 117, 4034–4043.
Roy, G., Placzek, E., Scanlan, T.S., 2012. ApoB-100-containing lipoproteins are major carriers of 3-iodothyronamine in circulation. J. Biol. Chem. 287, 1790–1800.
Saba, A., Chiellini, G., Frascarelli, S., Marchini, M., Ghelardoni, S., Raffaelli, A., Tonacchera, M., Vitti, P., Scanlan, T.S., Zucchi, R., 2010. Tissue distribution and cardiac metabolism of 3-iodothyronamine. Endocrinology 151, 5063–5073.
Sampaolo, S., Campos-Barros, A., Mazziotti, G., Carlomagno, S., Sannino, V., Amato, G., Carella, C., Di Iorio, G., 2005. Increased cerebrospinal fluid levels of 3,3′,5′-triiodothyronine in patients with Alzheimer's disease. J. Clin. Endocrinol. Metab. 90, 198–202.
Scanlan, T.S., 2009. Minireview: 3-Iodothyronamine (T1AM): a new player on the thyroid endocrine team? Endocrinology 150, 1108–1111.
Scanlan, T.S., Suchland, K.L., Hart, M.E., Chiellini, G., Huang, Y., Kruzich, P.J., Frascarelli, S., Crossley, D.A., Bunzow, J.R., Ronca-Testoni, S., Lin, E.T., Hatton, D., Zucchi, R., Grandy, D.K., 2004. 3-Iodothyronamine is an endogenous and rapid-acting derivative of thyroid hormone. Nat. Med. 10, 638–642.
Shabani, S., Farbood, Y., Mard, S.A., Sarkaki, A., Ahangarpour, A., Khorsandi, L., 2018. The regulation of pituitary-thyroid abnormalities by peripheral administration of levothyroxine increased brain-derived neurotrophic factor and reelin protein expression in an animal model of Alzheimer's disease. Can. J. Physiol. Pharmacol. 96, 275–280.
Smith, J.S., Kiloh, L.G., 1981. The investigation of dementia: results in 200 consecutive admissions. Lancet 1, 824–827.
Snead, A.N., Santos, M.S., Seal, R.P., Miyakawa, M., Edwards, R.H., Scanlan, T.S., 2007. Thyronamines inhibit plasma membrane and vesicular monoamine transport. ACS Chem. Biol. 2, 390–398.
Sui, L., Ren, W.-W., Li, B.-M., 2010. Administration of thyroid hormone increases reelin and brain-derived neurotrophic factor expression in rat hippocampus in vivo. Brain Res. 1313, 9–24.
Tecuatl, C., Herrrera-López, G., Martín-Ávila, A., Yin, B., Weber, S., Barrionuevo, G., Galván, E.J., 2018. TrkB-mediated activation of the phosphatidylinositol-3-kinase/Akt cascade reduces the damage inflicted by oxygen-glucose deprivation in area CA3 of the rat hippocampus. Eur. J. Neurosci. 47, 1096–1109.
Uryu, K., Laurer, H., McIntosh, T., Praticò, D., Martinez, D., Leight, S., Lee, V.M.-Y., Trojanowski, J.Q., 2002. Repetitive mild brain trauma accelerates Abeta deposition, lipid peroxidation, and cognitive impairment in a transgenic mouse model of Alzheimer amyloidosis. J. Neurosci. 22, 446–454.
Volpato, S., Guralnik, J.M., Fried, L.P., Remaley, A.T., Cappola, A.R., Launer, L.J., 2002. Serum thyroxine level and cognitive decline in euthyroid older women. Neurology 58, 1055–1061.
Yokota, M., Saido, T.C., Tani, E., Yamaura, I., Minami, N., 1996. Cytotoxic fragment of amyloid precursor protein accumulates in hippocampus after global forebrain ischemia. J. Cereb. Blood Flow Metab. 16, 1219–1223.
Zhang, F., Eckman, C., Younkin, S., Hsiao, K.K., Iadecola, C., 1997. Increased susceptibility to ischemic brain damage in transgenic mice overexpressing the amyloid precursor protein. J. Neurosci. 17, 7655–7661.
Zucchi, R., Accorroni, A., Chiellini, G., 2014. Update on 3-iodothyronamine and its neurological and metabolic actions. Front. Physiol. 5, 402.